Bulletin of the Czech Geological Survey, Vol. 77, No. 4, 313–320, 2002

Shock-induced phenomena in limestones in the quarry near Ronheim, the Ries Crater, Germany

ROMAN SKÁLA

Czech Geological Survey, Klárov 3, 118 21 Praha 1, Czech Republic; e-mail: skala@cgu.cz

A b s t r a c t. Shock-induced effects in Malmian limestone sequences sampled in the quarry near Ronheim in the southeastern rim of the Ries impact structure in Germany were studied using electron microscopy with local chemical microanalysis, X-ray powder diffraction, IR spectroscopy, stable isotope study and MAS NMR spectroscopy. The most pronounced deformation observed is a pervasive brecciation resulting in the formation of parautochthonous to completely allochthonous limestone megablocks (so-called "Schollen") on a megascopic scale. On a macroscopic scale, this process gives rise to monomict breccias (so-called "Gries"). The applied analytical methods also revealed the damage of the limestones on submicroscopic and atomic scales. The peaks in X-ray diffraction patterns are broadened due to increased domain size and microstrain. Bands in the MAS NMR spectra show also broadening – most probably due to the random shifts of CO_3^{2-} ions in the calcite crystal structure. The overall degree of shock-induced solid-state deformation is, however, low. No decomposition, stable isotope fractionation or melting occurring at high degrees of shock metamorphism were found. This allows to speculate on fast attenuation of peak shock pressure towards the crater rim in the most superficial regions of the target. Also the role of brittle behaviour of carbonates occurring in a relatively thin layer deposited over more competent crystalline basement revealing considerably higher degrees of shock metamorphism in large volumes must be taken into account in interpreting the low degree of shock metamorphism in the studied limestones.

A b s t r a k t. Ke studiu jevů vyvolaných šokovou metamorfózou v malmských vápencích z lomu poblíž Ronheimu na jv. okraji impaktové struktury Ries byla použita elektronová mikroskopie doprovázená lokální chemickou mikroanalýzou, rentgenová prášková difrakce, IČ spektroskopie, studium stabilních izotopů a MAS NMR spektroskopie. V megaskopickém měřítku je nejvíce zřejmým projevem šokové metamorfózy masivní brekciace, která dává vzniknout parautochtonním až zcela alochtonním blokům vápence (místně nazývaným "Schollen"). Makroskopicky tato brekciace rezultuje ve tvorbu monomiktních brekcií (tzv. "Gries"). Analytické metody použité při tomto studiu odhalily rovněž postižení vápenců v submikroskopickém a atomárním měřítku. Maxima v difrakčních záznamech jsou rozšířená a poukazují na zmenšení velikosti koherentně difraktujících domén a zvýšení mikropnutí. Rozšíření pásů v MAS NMR spektrech je interpretováno jako důsledek poziční neuspořádanosti iontů CO_3^{2-} v krystalové struktuře kalcitu. Nicméně, celkový stupeň šokové metamorfózy je nízký. Nepodařilo se zjistit produkty rozkladu kalcitu nebo jeho taveniny ani se neprokázala izotopová frakcionace, tj. jevy, které by indikovaly vyšší stupeň šokového postižení. To ukazuje na rychlé zeslabení vlivu šokové vlny na povrchové sekvence na okraji impaktového kráteru. Stejně důležitou roli hraje pravděpodobně mechanická křehkost karbonátů, které se vyskytují jen jako relativně tenká vrstva uložená na krystaliniku, jež je pevnější a jeví mnohem vyšší stupeň postižení ve velkých objemech.

K e y w o r d s: impact structures, shock metamorphism, limestone, calcite, cell dimensions, Ries Crater, X-ray diffraction, infra-red spectroscopy

Introduction

Shock metamorphism due to a hyper-velocity impact of a cosmic body is known to produce specific permanent diagnostic features in many rock-forming minerals. These changes are collectively called shock metamorphic effects (see, e.g. French 1998 and references therein). Major attention has traditionally been paid to shock metamorphic effects in framework silicates – quartz and feldspars – because they represent the most widespread minerals in terrestrial crustal rocks and can be used for estimates of the degree of shock metamorphism (Stöffler 1972, 1974; Stöffler and Langenhorst 1994). Olivine is equally important diagnostic mineral for the recognition and classification of shock metamorphism in stony meteorites (Stöffler et al. 1991 and Scott et al. 1992). Surprisingly, studies of terrestrial impact structures have only rarely been devoted to carbonates occurring in them and to potential shock effects, though carbonates have been demonstrated to be present in about 30% of known terrestrial impact structures (Kieffer and Simonds 1980, Lange and Ahrens 1986). Consequently, our knowledge of shock-induced phenomena in the rock-forming carbonates is not systematic, and only a few papers addressed some particular aspects. To name at least some examples of papers dealing with natural samples: Barber and Wenk (1979) studied limestones from the Ries by TEM, Martinez et al. (1994) determined stable isotope composition in limestones and dolostones of the Haughton impact structure, Graup (1999), Jones et al. (2000), and Osinski and Spray (2001) published reports on finds of carbonate melts from the craters of Ries, Chicxulub and Haughton. In addition to these papers, experimentally shock-loaded calcites and dolomites were recently investigated also by, e.g. Bell (1997), Bell et al. (1998), Ivanov et al. (2000), Langenhorst et al. (2000), Martinez et al. (1995) and Skála et al. (1999, 2000).

The present paper focuses on detailed mineralogical study of limestones from the locality near Ronheim in the southeastern rim part of the Ries impact structure. The aim of the paper is to determine the degree of shock metamorphism in these rocks and also to demonstrate the geological reasons for the development of the observed shock-induced features in the material.

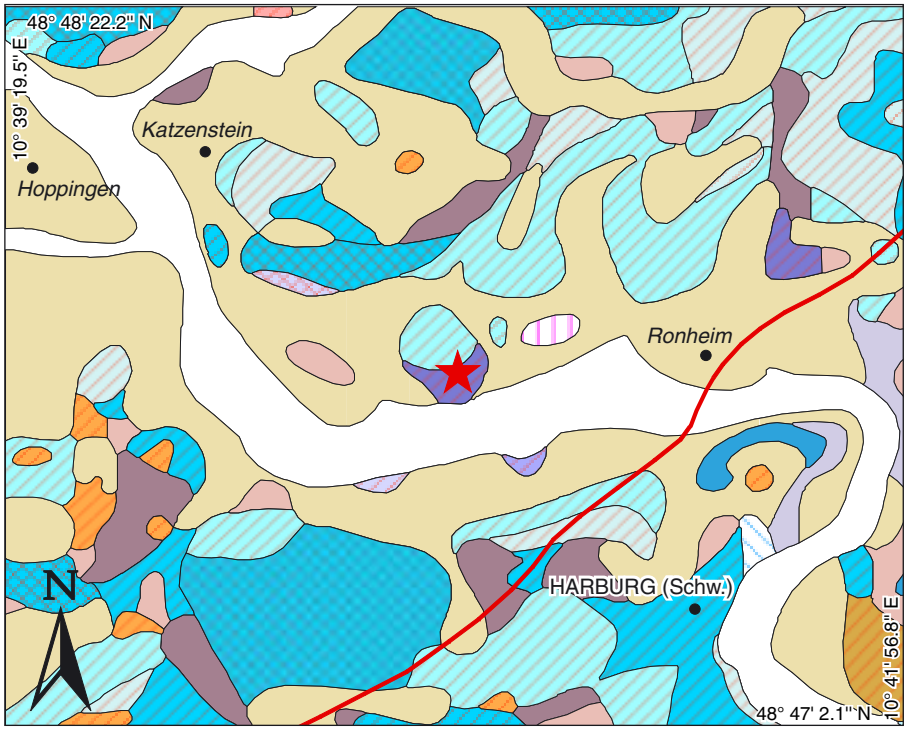

Fig. 1. Geological map of the area studied. The solid red line delineates the crater rim. The red star shows the location of the quarry west of the village. Blue colours indicate Malmian limestone outcrops. Violet indicates the Bunte Breccia outcrops. Shades of brown colour determine the distribution of Triassic sediments. Red diagonal hachure marks parautochthonous strata whereas cross-hatched areas correspond to completely allochthonous sequences. Modified according to the GLA map of the Ries crater 1 : 50 000 (Bayerisches Geologisches Landesamt, 1999).

Geological setting and samples

The Ries crater is located approximately in the centre of a triangle delimited by the cities of Munich, Nürnberg and Stuttgart, about 110 km NW of Munich. It is a flat-bottomed, more or less circular morphological depression 22 to 23 km in diameter with typical altitude of 410–430 m above sea level. It lies in the hilly region between geographical units of the Swabian and Franconian Alb.

Based on the morphological and surface geological data, Pohl et al. (1977) subdivided the crater and its impact formations into the following major concentric zones and structural elements: central basin, inner ring, zone of megablocks, tectonic rim of the crater, Vorries continuous deposits, and zone of distal ejecta. The limestone quarry sampled is located W of the village of Ronheim (geographic coordinates: N 48° 47’ 41.1”, E 10° 40’ 28.8”) just at the boundary of megablock and tectonic rim zones. For location of the quarry and sketch of geological setting see a section from a geological map of the Ries crater to scale 1 : 50 000 (Bayerisches Geologisches Landesamt, 1999) shown in Fig. 1. Generally, all megabreccia limestone materials are known to display only low degree of shock metamorphism (shock stages 0 and only rarely Ia). The mode of brecciation and fracturing of these blocks, however, is characteristic – limestones commonly reveal brittle fracturing (Hüttner and Schmidt-Kaler 1999a, b). On the other hand, also extremely shocked carbonates are reported to occur in the Ries crater – Graup (1999) described shock-melted carbonates from many suevite outcrops throughout the crater.

The samples taken represent the Malmian bedded limestones, their breccias, and thin mylonite (slickenside) beds developed along some of the bedding planes. As a standard reference unshocked material, a sample of the Malmian Solnhofen lithographic limestone was used. The list and description of the studied samples are given in Table 1.

Table 1. A list of samples used in this study with their macroscopic description.

Sample	Locality	Description
RS-01	Solnhofen	Unshocked thin-bedded ochre coloured lithographic Solnhofen limestone of Upper Malmian age. The beds are about 1 cm thick. Bedding planes are sometimes covered by black dendrites of ?Mn/Fe-oxides/hydroxides
RS-19	Ronheim	Slickenside mylonite from between solid limestone beds
RS-20	Ronheim	Up to 1 cm thick layer of limestone cataclasite of light grey colour from between thicker brecciated beds of limestone; both surfaces are covered by strongly striated slickenside-like material of dark brown, green-brown or grey colour with silky lustre
RS-21	Ronheim	Greyish white fractured cm-sized clasts of massive limestone from monomict breccia; with thin beige to rusty-coloured varnish on the surface. Batch A represents compact massive limestone with rare striations; batch B is a heavily brecciated to mylonitized carbonate matter from boundary of two limestone beds associated with incipient development of slickensiding
RS-22	Ronheim	Monomict breccia of massive clayey limestone of light grey colour on fresh saw plane, weathered surface is rusty beige coloured. Open fissures in the rock are up to 0.5 mm wide. Individual angular to subangular clasts are of highly variable size ranging from millimetres to several centimetres but no fine-grained matrix occurs

Experimental studies

Besides the field megascopic and macroscopic characteristics of the locality, an attempt was made to study microscopic and submicroscopic properties. Due to extremely fine-grained nature of the sampled rocks, the use of optical microscopy was not suitable and other experimental methods had to be applied. These experimental techniques employed to study shock-induced effects in limestone materials sampled in the quarry near Ronheim include electron microscopic study, X-ray powder diffraction, IR spectroscopy, stable isotope study and MAS NMR spectroscopy.

Secondary electron images of sample surfaces have been taken using electron microscopes TESLA BS 340 and CamScan IV at the Czech Geological Survey in Prague (CGS). The samples studied were sputtered with a Pd-Au alloy and images were collected using either photographic (TESLA) or electronic (CamScan – ISIS) techniques. Photographs taken with the TESLA SEM were subsequently converted to electronic files using a flatbed scanner.

Chemical composition was determined in polished thin sections using the Oxford Link ISIS 300 energy-dispersive system (with an ultra-thin detector window) connected to the CamScan IV microscope (at the CGS). Accelerating voltage was 15 kV and sample current was set to 2.5 nA. Spectrum acquisition time was 40 s. Studied carbonates were analysed for Ca, Mg, Fe and Mn only. Other elements were found to be below detection limit of the used equipment. The standards used for element quantification were synthetic $CaSiO_3$, Mg_2SiO_4, Fe_2SiO_4, and Mn_2SiO_4, respectively.

X-ray powder diffraction patterns were acquired on the Philips X'Pert MPD diffractometer at the Czech Geological Survey in Prague. The diffractometer was operated in reflecting Bragg-Brentano geometry with Cu$K_{\alpha 1 \alpha 2}$ radiation. Samples were placed atop low-background silicon sample holders and step-scanned in the range of 3 to 65 °2θ with 0.1 °2θ step for phase identification and 15 to 145 °2θ with 0.02 °2θ step for detail peak width and unit cell dimensions analysis. Qualitative phase analysis has been performed with the Bede Search/Match program and ICDD PDF2 database release of 2001. For single peak profile fitting XFit program (Coelho and Cheary 1997) was used. Subsequently, diffraction indices were assigned to refined peak positions based on the theoretical powder pattern generated from the crystal structure data of Effen-

Fig. 2. Slight bending is well observable in the limestone block because mylonite zones formed along original bedding planes to accommodate the motion in otherwise competent and brittle limestones. It is necessary to stress that outside the crater all Malmian limestone sequences are essentially flat-lying, free of any deformations.

Fig. 3. A detail of various brittle deformations occurring in limestones in the quarry west of Ronheim. The most pronounced effects seen in this photograph are the formation of mylonite zones along original bedding planes and also incipient formation of monomict breccias at some places.

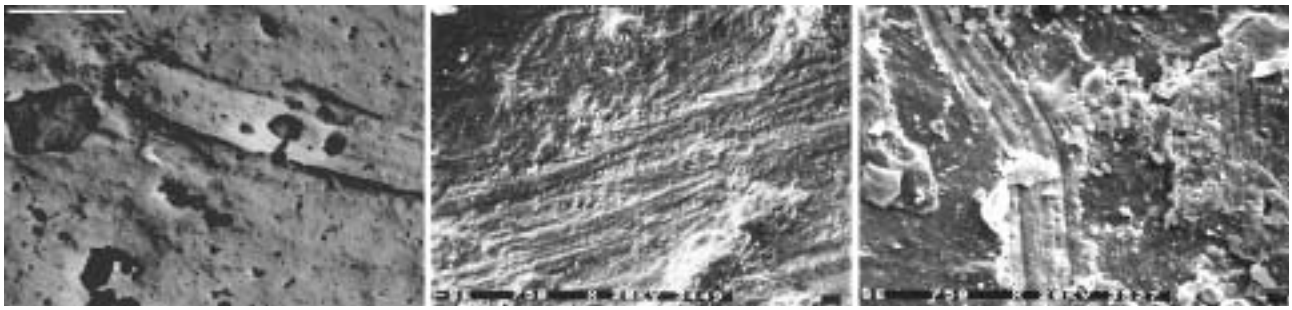

Fig. 4. Scanning electron microscope images of surfaces of highly striated slickenside material developed on about 1 cm thick layer of limestone cataclasite occurring between thicker brecciated beds of limestone. Both relatively shallow striations and very marked grooves are present. Generally, the striation directions are parallel (a), but some also converge (b) demonstrating a more complex and multiple-stage movement. Rarely, also curvilinear striations were observed (c).

berger et al. (1981) by the program LAZY PULVERIX (Yvon et al. 1977) and unit cell dimensions calculated applying a least-square program by Burnham (1962).

Infrared spectra were collected using the Nicolet spectrometer at the Institute of Chemical Technology in Prague. Weighed amounts of powdered samples (about 20 mg) were pressed into KBr discs. The spectra were collected to cover the wavenumber range of 400-4000 cm^{-1}. Positions and widths of the spectral absorption bands were evaluated with the use of an asymmetric Pearson VII function.

The ^{13}C NMR spectra were measured at Inova UNITY 400 NMR (resonance frequency ^{13}C 100.57 MHz) spectrometer using 7 mm CP MAS probe and silicon nitride rotors at the Faculty of Science, Charles University, Prague. The rotation frequency of the sample was approximately 4 kHz. The 90 degree pulse (duration 5.7 μs) and relaxation delay 100 s were used. In the time domain 2 k data points were acquired, the FID was not zero filled. For each sample approximately 128 transients were acquired. The Fourier transformation to the frequency domain was performed without multiplication with weighing functions. Hexamethylbenzene was used as an external reference standard. The half-widths $\Delta\nu_{1/2}$ of the CO_3^{2-} signals were obtained by Varian software in the frequency domain.

For carbon and oxygen stable isotope determination, the carbonate samples studied were decomposed by 100% H_3PO_4 under vacuum and released CO_2 gas was measured using a Finnigan MAT 251 mass spectrometer at the Stable Isotope Lab of the Czech Geological Survey in Prague.

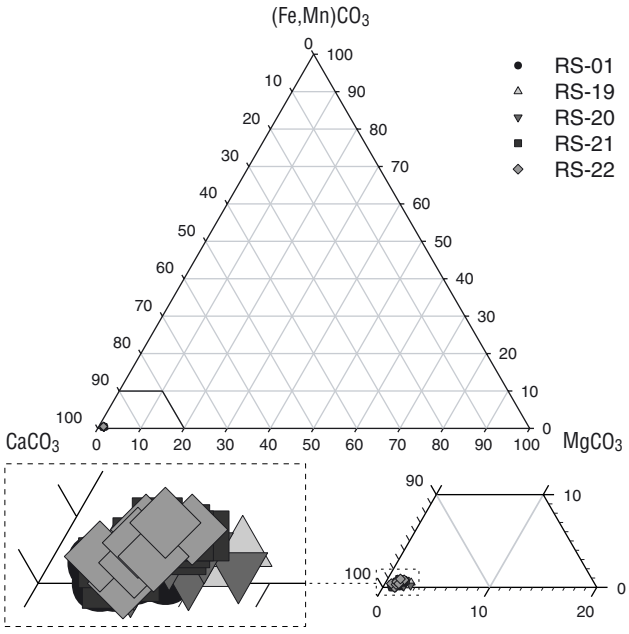

Fig. 5. Chemical composition of shocked calcite from limestones sampled at the Ronheim quarry compared to unshocked Solnhofen limestone plotted as molar percentages of $CaCO_3$, $MgCO_3$ and (Fe, Mn)CO_3. Note the tight clustering of all data with the entire compositional range corresponding to some 98 to 99 mol% $CaCO_3$ and 1 to 1.5 mol% $MgCO_3$.

Results and interpretations

The most pronounced megascopic effect encountered in this quarry is the detachment of the whole large blocks of Malmian bedded limestone off the basement which is demonstrated by varying dips of bedding planes and also by their bending at some places (Fig. 2) although all Malmian limestone sequences are essentially flat-lying outside the crater. Furthermore, the megablock is divided into several smaller blocks, which are mutually displaced and rotated.

Particular individual blocks are deformed to various degrees ranging from simple bending of bedding planes to massive cataclasis resulting in the formation of monomict breccias – so-called "Gries" (see, e.g. Pohl et al. 1977) – and to the development of mylonite zones along bedding planes or pre-existing weakened domains (Fig. 3). The monomict breccias contain angular to subangular clasts of various dimensions ranging from millimetres to several decimetres in size. Mylonites are characterized by the presence of slickenside surfaces decorated by striations revealing the movement directions of the individual blocks.

Scanning electron microscope images revealed the presence of a multitude of striations of varying dimen-

Table 2. Empirical formulae coefficients for calcite in the studied limestones from the Ronheim quarry compared to the Solnhofen limestone composition (sample RS-01).

Sample	Ca	Mg	Fe	Mn
RS-01	0.986(3)	0.012(3)	0.002(1)	ND
RS-19	0.981(5)	0.014(5)	0.004(2)	ND
RS-20	0.984(5)	0.013(5)	0.002(2)	0.001(1)
RS-21	0.984(6)	0.012(4)	0.004(3)	0.000(1)
RS-22	0.984(4)	0.011(2)	0.004(2)	0.001(1)

Notes: The data given represent arithmetic means from 15 individual point analyses; the values in parentheses stand for 1 sigma; ND means that the content was below detection limit.

sions, appearance and mutual relationships. There are both relatively faint, low-relief but abundant parallel striations occurring in sets (Fig. 4a) and marked, much deeper furrows with uplifted rims (Fig. 4b). Usually, striations are straight, but some curvilinear striations were also found. Generally, the striation directions are parallel, however, some exceptions exist and several converging or even intersecting striations or their sets were noticed. The orientation of striations shows the direction of both principal movements in the phase of crater formation and subsequent shifts due to crater modification stage.

Qualitative phase analysis using powder X-ray diffraction revealed the dominant presence of calcite in the samples studied. Subordinate phases were quartz and clay minerals. This phase composition was also confirmed by results of chemical local micro-analyses performed using the microprobe. Calcite composition is more or less uniform – contents of other than calcite end-members are limited to less than 5 mol%. Mean chemical composition of the studied samples is given in Table 2 as empirical formulae. Clustering of the data is also well demonstrated in the compositional triangular diagram $CaCO_3$-$MgCO_3$-$(Fe,Mn)CO_3$ in Fig. 5. Apparently, all electron microprobe data yield more or less constant composition indicating the presence of calcite with small admixture of magnesite end-member but no calcite decomposition products or new shock-induced phase assemblages were observed at the spatial resolution of the electron microprobe beam (i.e. ~ 1 μm).

A detailed study of powder X-ray diffraction data showed a slight peak broadening in the samples from the quarry near Ronheim compared to unshocked Solnhofen limestone. This broadening is not obvious from qualitative visual inspection of the powder patterns acquired, as shown in Fig. 6. Instead, a quantitative approach has to be applied to evaluate the degree to which peaks become broadened compared to unshocked standard. Half-widths of the peaks were plotted against the diffraction angle for sample RS-19 that revealed the highest peak broadening and for the unshocked Solnhofen limestone for clarity in Fig. 7 only. Figure 8 summarizes the data on broadening for all the samples investigated. Peak broadening is defined here as the ratio $100 \times (W_e - W_s)/W_s$, where W_e is the half-width of the sample and W_s is the half-width of

Table 3. Unit-cell parameters refined from individual peak positions.

Sample	a (Å)	c (Å)	V (Å^3)	c/a
RS-01	4.9879(3)	17.055(1)	367.48(5)	3.4193(3)
RS-19	4.9856(4)	17.042(2)	366.87(8)	3.4183(5)
RS-20	4.9863(4)	17.045(2)	367.02(7)	3.4183(4)
RS-21A	4.9866(4)	17.051(2)	367.21(7)	3.4194(4)
RS-21B	4.9865(3)	17.055(1)	367.28(6)	3.4203(4)
RS-22	4.9869(4)	17.047(2)	367.14(8)	3.4183(5)

the standard reference specimen. It is generally known that peak broadening might be due to a decrease in size of coherently diffracting domains or because of inducing microstrain or a combination of both. To evaluate the effects of both contributions, a fundamental approach implemented in the XFit program of Coelho and Cheary (1997) was applied. Unfortunately, all profiles appeared when treated with pseudo-Voigt function in FullProf.2k program (Rodríguez-Carvajal 1990, 2002), super-Lorentzian, and, consequently, the results of fundamental approach are rather qualitative. Nevertheless, refining microstrain and domain-size contributions showed the dominance of the latter in broadening of peaks in the powder pattern acquired.

In addition to peak broadening, unit-cell dimensions were also refined from peak positions. The unit-cell parameters are summarized in Table 3. Unit-cell edges and volumes are also compared diagrammatically in Fig. 9. Unit-cell parameters are slightly lower for shocked calcite, the highest difference being observed for sample RS-19, which is in accordance with the data on peak broadening. The volume of the unit-cell is lower by as much as 0.2 rel.% compared to that of calcite in the Solnhofen limestone; this is just opposite trend than that observed in quartz (e.g. Stöffler and Langenhorst 1994). This change might indicate that hysteresis occurs in the crystal structure of calcite upon release from a shock compression and

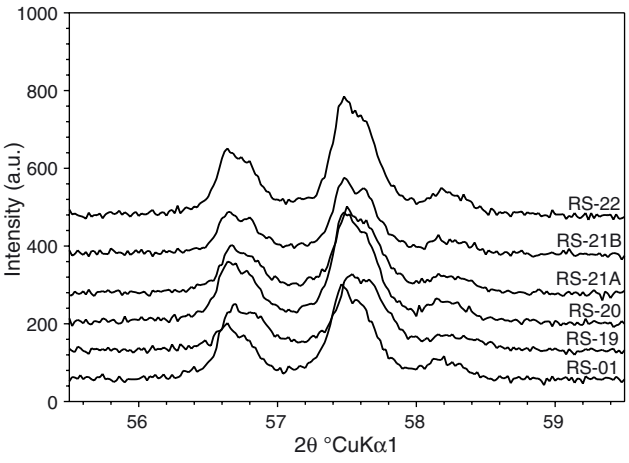

Fig. 6. Comparison of powder patterns of the studied limestones. Shown is the region between 55.5 and 59.5 °2θ Cu$K_{\alpha 1}$. The peaks, from the left to right, correspond to reflections 211, 122, and 1.0.10 of calcite. The broadening is not even that pronounced as in carbonates experimentally shock-loaded at only mild shock levels. Rather than clear broadening, a loss of the resolution is obvious in some patterns (e.g. RS-19 and RS-21A).

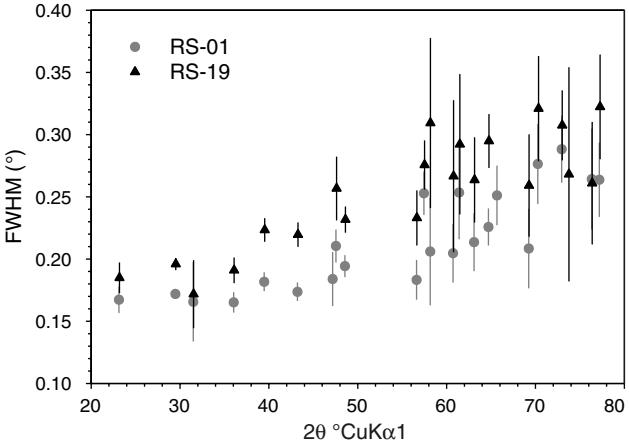

Fig. 7. Plot of FWHM vs. diffraction angle showing the peak half-width of sample RS-19 compared to that of unshocked standard. Peaks of mechanically comminuted limestone of sample RS-19 are distinctly broader than those of the Solnhofen limestone. Only these two samples are shown for clarity, others plot just in between the half-width data represented by the two patterns.

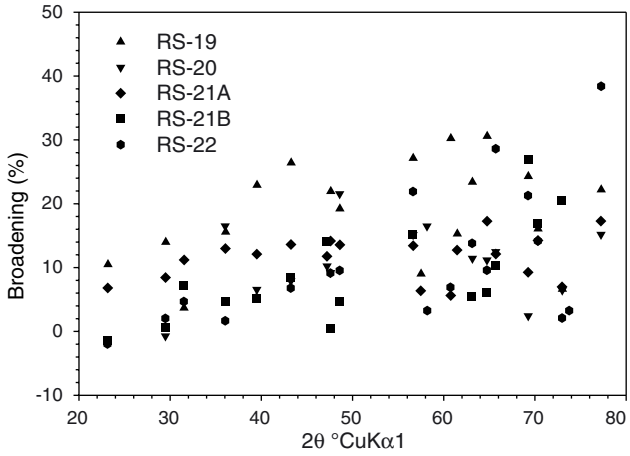

Fig. 8. Peak broadening in X-ray powder diffraction patterns in comparison to unshocked Solnhofen limestone. Peaks were reliably fit only in the region below 80 °2θ, therefore no high-angle data are presented. The maximum broadening is observed in sample RS-19.

that the unit-cell does not relax completely to the state before an impact.

The IR spectra of unshocked and shocked materials do not reveal any significant differences in band positions or widths. They indicate, in agreement with powder X-ray diffraction and microprobe data, the presence of quartz, feldspars and clay minerals in addition to calcite.

In the MAS NMR spectra, the values of chemical shift and half-width of peaks were measured. The chemical shifts of ^{13}C in calcite samples are approximately 167 ppm, i.e., in the region expected for C=O groups. The same chemical shift was found for chemically pure $CaCO_3$ (Fluka). The numerical value of the chemical shift of ^{13}C, varying between 167 to 169 ppm among individual samples, does not appear to be a useful parameter to judge the shock-induced deformation.

Contrary to that, the linewidths $\Delta\nu_{1/2}$ of ^{13}C NMR signals differ and appear to correlate with the pressure that the sample was subjected to. The $\Delta\nu_{1/2}$ increases with the increasing shock pressure. The $\Delta\nu_{1/2}$ of the Solnhofen limestone sample was found to be ~ 45 Hz, while a more that five-fold increase in $\Delta\nu_{1/2}$ was observed for the shocked samples. The lineshape of the ^{13}C NMR signal remains roughly the same for all the samples studied without significant dependence on the shock pressure.

The change in $\Delta\nu_{1/2}$ of ^{13}C NMR resonance reflects a change in electron density around the carbon atom in the crystal structure caused by a passage of shock and rarefaction waves. Thus, the ^{13}C atom is shielded by different electron density than in the ideal calcite structure. The chemical shift of ^{13}C changes with the shielding constant. The increase in $\Delta\nu_{1/2}$ is governed by chemical shift dispersion rather than relaxation time change. The change in electron density around ^{13}C can be caused either by random shifts of CO_3^{2-} ions in the crystal structure or by deformation of formerly planar CO_3^{2-}. The shift of CO_3^{2-} ion in the crystal structure seems to be more probable, taking into account the results of XRD and IR spectroscopy.

The carbon and oxygen isotopic composition of calcite of brecciated massive limestones and cataclasites from Ronheim were found to be tightly clustered around $\delta^{18}O_{SMOW}$ = 27.9 ‰ and $\delta^{13}C_{PDB}$ = 2.2 ‰. Such isotopic composition of carbon and oxygen corresponds to carbonates deposited from normal Jurassic seawater (Veizer et al. 1999). Apparently, no isotopic fractionation comparable to that found in carbonate materials from the Haughton impact structure (Martinez et al. 1994) occurred in the studied samples. This supports the idea of relatively low peak shock pressures to which the samples had been subjected.

Conclusions

On megascopic and macroscopic scale, brittle behaviour of carbonates in the quarry near Ronheim is well demonstrated. Fracturing on all scales, detachment of individual beds along bedding planes associated with development of slickenside layers and formation of monomict breccias dominate. Bending of limestone beds is also frequent, however, it is always accompanied with strong fracturing perpendicular to bedding, which compensates for this plastic deformation. The direction of movement of blocks or individual limestone beds within them can be followed by the study of striations pervasively developed on slickensides formed along these bedding planes. A detailed SEM study revealed that the mutual shifts of blocks and/or beds need not necessarily be a simple one-stage process; curvilinear or converging and intersecting striations document the relatively complex and multi-stage movements associated in some way most probably with individual stages of crater formation and modification.

X-ray diffraction study shows peak broadening chiefly

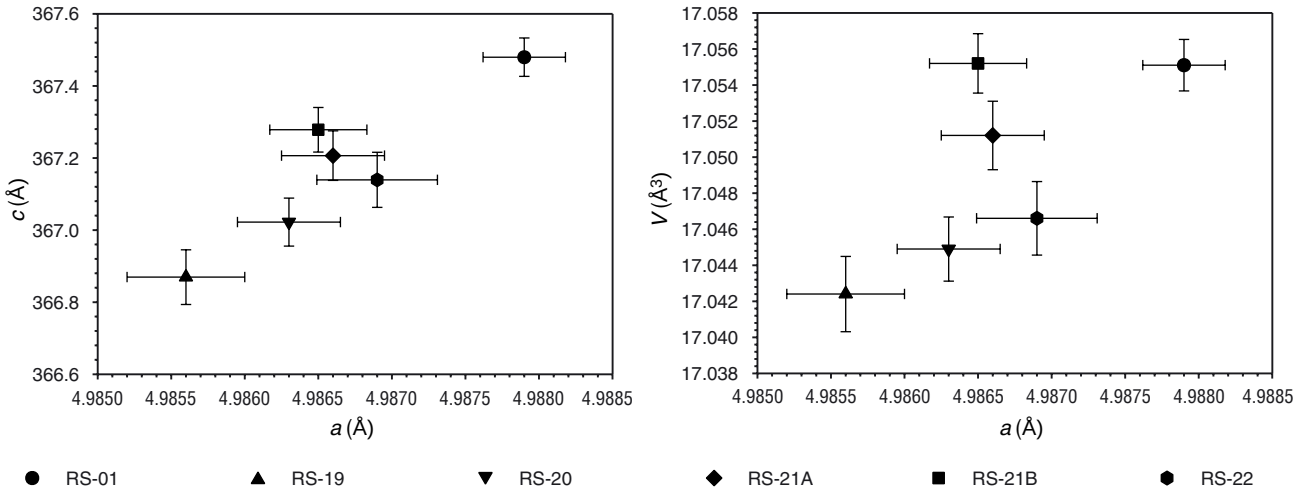

Fig. 9. Unit-cell dimensions of the studied calcite. Shocked samples reveal a decrease in unit-cell volume and cell edge *a* compared to the unshocked reference material. The highest difference was found for sample RS-19, which agrees also with the maximum broadening of peaks in the diffraction pattern of this material.

due to a decrease in crystallite size induced by submicroscopic comminution of shocked carbonates. Unit-cell volume decreases with the expected increasing degree of shock metamorphism and most probably accounts for a hysteresis of calcite during shock compression.

The study of chemical composition using electron microprobe did not confirm any decomposition of shocked carbonates on the scale of ca. 1 μm, indicating relatively low pressures and temperatures attained during the passage of a shock and rarefaction wave through them. Likewise, stable isotope composition of shocked carbonates reveals no change in comparison to literature data for Jurassic seawater carbonates thus confirming very low degree of shock metamorphism which produced no fractionation of the kind observed in highly shocked carbonate materials from the Haughton impact structure or during the shock-loading experiments (Boslough et al. 1982, Martinez et al. 1994, 1995).

Interesting is the comparison with shock-induced phenomena encountered in carbonate rocks occurring in the Haughton impact structure on the Devon Island in the Northwest Territories, Canada. A wide range of shock-induced deformations was observed in shocked limestones and dolomites including relatively frequent melting of carbonates (Martinez et al. 1994, Osinski and Spray 2001). The Haughton structure is about the same size as the Ries crater, however, the shock phenomena in carbonate sequences of the Canadian structure are more pronounced and some of the shock-induced features present in the Haughton structure are rare or completely absent in the Ries crater. The most probable explanation of these discrepancies is the difference in vertical stratification of the two target areas. Whereas in the area of the Ries impact structure, the pre-impact stratigraphy was dominated by crystalline rocks topped by a relatively thin sedimentary layer containing less than 350 m of carbonates (e.g. Graup 1999), the thickness of carbonate sequences at the Haughton crater is estimated to exceed 1500 m prior to the impact. Consequently, it is obvious that higher degrees of shock metamorphism associated with carbonate melting described from Ries by Graup (1999) are limited to lithologies occurring originally in the centralmost parts of the Ries structure while most of peripheral carbonate occurrences are shocked only weakly. Necessarily, the degree to which the megablock material near Ronheim situated on the crater rim has been shocked can be expected to be relatively low, resulting in only brittle deformations.

Generally, it is possible to conclude that the attenuation of shock pressure in the most superficial parts of the target near the transient crater rim was extremely fast. This is even enhanced by the brittle response of the uppermost portion of target materials, which detached off the more competent target rocks and consequently became shocked to a considerably lower degree than in the case of a homogeneous target.

Acknowledgements. The samples studied and most of the results have been acquired for purposes of the research carried out within the project of the Grant Agency of the Czech Republic No. 205/95/0980. The author also thanks Ananda Gabašová (Czech Geological Survey, Prague) for taking a part of the SEM images, Miroslava Novotná (Institute of Chemical Technology, Prague) for collecting IR spectra, Jan Rohovec (Faculty of Science, Charles University, Prague) for measurement of MAS NMR spectra, and Karel Žák (Czech Geological Survey, Prague) for acquisition of stable isotope data. Gisela Pösges of the Rieskratermuseum at Nördlingen kindly provided unshocked Solnhofen limestone sample used as a standard for some analytical techniques.

References

Barber D. J., Wenk H. R. (1979): On geological aspects of calcite microstructure. Tectonophysics 54, 45–60.

Bayerisches Geologisches Landesamt (1999): Geologie des Rieses 1 : 50 000. GLA, München. CD-ROM.

Bell M. S. (1997): Experimental shock effects in calcite, gypsum, and quartz. Meteoritics Planet. Sci. 32, Supplement, A11.

Bell M. S., Hörz F., Reid A. (1998): Characterization of experimental shock effects in calcite and dolomite by X-ray diffraction. Lunar Planet. Sci. IXXX, Abstract #1422 (CD-ROM).

Boslough M. B., Ahrens T. J., Vizgirda J., Becker R. H., Epstein S. (1982): Shock-induced devolatilization of calcite. Earth Planet. Sci. Lett., 61, 166–170.

Burnham C. W. (1962). Lattice constant refinement. Carnegie Institution of Washington Yearbook, 61, 132–135.

Coelho A. A., Cheary R. W. (1997): X-ray Line Profile Fitting Program, XFIT. School of Physical Sciences, University of Technology, Sydney, New South Wales, Australia. ftp://ftp.minerals.csiro.au/pub/xtallography/koalariet (program).

Effenberger H., Mereiter K., Zemann J. (1981): Crystal structure refinements of magnesite, calcite, rhodochrosite, siderite, smithonite, and dolomite, with the discussion of some aspects of the stereochemistry of calcite type carbonates. Z. Kristallogr., 156, 233–243.

French B. M. (1998): Traces of Catastrophe: A Handbook of Shock-Metamorphic Effects in Terrestrial Meteorite Impact Structures. LPI Contribution No. 954, Lunar and Planetary Institute, Houston.

Graup G. (1999): Carbonate-silicate liquid immiscibility upon impact melting, Ries Crater, Germany. Meteoritics and Planet. Sci. 34, 425–438.

Hüttner R., Schmidt-Kaler H. (1999a): Die geologische Karte des Rieses 1 : 50 000. Geologica Bavarica, 104, 7–76.

Hüttner R., Schmidt-Kaler H. (1999b): Meteoritenkrater Nördlinger Ries. Wanderungen in die Erdgeschichte (10). Pfeil, München.

Ivanov B. A., Langenhorst F., Deutsch A., Hornemann U. (2000): How strong was shock-induced CO_2 degassing in the K/T event? In Catastrophic Events and Mass Extenctions: Impacts and Beyond, LPI Contribution No. 1053, Lunar and Planetary Institute, Houston, 80–81.

Jones A. P., Claeys P., Heuschkel S. (2000): Impact melting of carbonates from the Chicxulub crater. In: Gilmour I., Koeberl C. (eds) Impacts and the Early Earth. Lecture Notes in Earth Sciences 91, Springer Verlag, Berlin, pp. 343–362.

Kieffer S. W., Simonds C. H. (1980): The role of volatiles and the lithology in the impact cratering process. Rev. Geophys. Space Phys., 18, 143–181.

Lange M. A., Ahrens T. J. (1986): Shock-induced CO_2 loss from $CaCO_3$; implications for early planetary atmospheres. Earth Planet. Sci. Lett., 77, 409–418.

Langenhorst F., Deutsch A., Ivanov B. A., Hornemann U. (2000): On the shock behavior of $CaCO_3$: Dynamic loading and fast unloading experiments – modeling – mineralogical observations. Lunar Planet. Sci. XXXI, Abstract #1851 (CD-ROM).

Martinez I., Agrinier P., Schärer U., Javoy M. (1994): A SEM-ATEM and stable isotope study of carbonates from the Haughton impact crater, Canada. Earth Planet. Sci. Lett., 121, 559–574.

Martinez I., Deutsch A., Schärer U., Ildefonse Ph., Guyot F., Agrinier P. (1995): Shock recovery experiments on dolomite and thermodynamical modelling of impact induced decarbonization. J. Geophys. Res., 100, 15465–15476.

Osinski G. R., Spray J. G. (2001): Impact-generated carbonate melts: evidence from the Haughton structure, Canada. Earth Planet. Sci. Lett., 194, 17–29.

Pohl J., Stöffler D., Gall H., Ernstson K. (1977): The Ries impact crater. In: Roddy D. J. et al. (eds) Impact and Explosion Cratering. Pergamon Press, New York, pp. 343–404.

Rodríguez-Carvajal J. (2002): FullProf.2k. Rietveld, Profile Matching & Integrated Intensities Refinement of X-ray and/or Neutron Data (powder and/or single-crystal). Laboratoire Léon Brillouin, Centre d'Etudes de Saclay, Gif-sur-Yvette Cedex, France. ftp://charybde.saclay.cea.fr/pub/divers/fullp (program).

Rodríguez-Carvajal J. (1990): FULLPROF: A program for Rietveld Refinement and Pattern Matching Analysis. Abstracts of the Satellite Meeting on Powder Diffraction of the XVth Congress of the IUCr. Toulouse, 127.

Scott E. R. D., Keil K., Stöffler D. (1992): Shock metamorphism of carbonaceous chondrites. Geochim. Cosmochim. Acta, 56, 4281–4293.

Skála R., Hörz F., Jakeš P. (1999): X-ray powder diffraction study of experimentally shocked dolomite. Lunar Planet. Sci. XXX, Abstract #1327 (CD-ROM).

Skála R., Matějka P., Hörz F. (2000): Experimentally shocked dolomite – a Raman spectroscopic study. Lunar Planet. Sci. XXXI, Abstract #1567 (CD-ROM).

Stöffler D. (1972): Deformation and transformation of rock-forming minerals by natural and experimental shock processes. I. Behavior of minerals under shock compression. Fortschr. Mineral., 49, 50–113.

Stöffler D. (1974): Deformation and transformation of rock-forming minerals by natural and experimental shock processes. II. Physical properties of shocked minerals. Fortschr. Mineral., 51, 256–289.

Stöffler D., Langenhorst F. (1994): Shock metamorphism of quartz in nature and experiment: I. Basic observation and theory. Meteoritics, 29, 155–181.

Stöffler D., Keil K., Scott E. R. D. (1991): Shock metamorphism of ordinary chondrites. Geochim. Cosmochim. Acta, 55, 3845–3867.

Veizer J., Ala D., Azmy K., Bruckschen P., Buhl D., Bruhn F., Carden G. A. F., Diener A., Ebneth S., Godderis Y., Jasper T., Korte Ch., Pawellek F., Podlaha O. G., Strauss H. (1999): $^{87}Sr/^{86}Sr$, $\delta^{13}C$ and $\delta^{18}O$ evolution of Phanerozoic seawater. Chemical Geology, 161, 59–88.

Yvon K., Jeitschko W., Parthé E. (1977): LAZY PULVERIX, a computer program for calculating X-ray and neutron diffraction powder patterns. J. Appl. Crystallogr., 10, 73–74.

Handling editor: Jan Pašava

RECENZE – REVIEW

I. Chlupáč – R. Brzobohatý – Z. Stráník – J. Kovanda (2002): *Geologická minulost České republiky.* Academia, Praha, 436 stran, 238 obr.

Téměř po dvaceti letech vyšla nová geologie Českého masivu, jejímž autorem je Ivo Chlupáč se spolupracovníky R. Brzobohatým, Z. Stránikem a J. Kovandou. Kniha o rozsahu 436 stran zaujme čtenáře již svou formou – je po vydavatelské stránce velmi dobře zpracovaná, včetně graficky poutavé obálky, doprovázena nezvykle velkým množstvím grafů, mapek, tabulek a kvalitních fotografií (celkem 238), které podstatně přispívají k oživení, přehlednosti i porozumění textu. Jde o obrázky v mnoha případech dosud nezveřejněné a někdy již neopakovatelné (např. z archivu J. Svobody); převažují však autorovy snímky a kvalitní fotografie zkamenělin a minerálů od J. Dudy, J. Bruthansové a dalších.

Dílo je dokladem velkých zkušeností autora i jeho spolupracovníků, je psáno čtivě, takže zaujme vysokoškolského studenta (kniha bude zcela jistě využívaná jako velmi kvalitní učebnice historické a do jisté míry i regionální geologie ČR), poučeného laika i sběratele. Dílo lze však rovněž doporučit i úzkým specialistům – prakticky všem našim geologům –